EurJOC
European Journal of Organic Chemistry

Full Papers
doi.org/10.1002/ejoc.202100097

Chemistry Europe
European Chemical Societies Publishing

Gallium(III) Corrole Complexes as Near-Infrared Emitter – Synthesis, Computational and Photophysical Study

Michael Haas,[a] Dominik Krisch,[a] Sabrina Gonglach,[a] Matthias Bechmann,[a] Markus C. Scharber,[b] Martin Ertl,[c] Uwe Monkowius,[c] and Wolfgang Schöfberger*[a]

This work is dedicated to Professor Norbert Müller on the occasion of his 65th birthday.

We report on the chemical synthesis and characterization of free-base A_2B- and A_3-*meso*-TIPS ethynyl corroles, which serve as a precursor for metalation with gallium(III)chloride and subsequent in-situ sila Sonogashira cross-coupling reaction. Under ambient conditions and with a common catalyst system the reaction with different aryliodides proved to be successful. Compared to the well-known Ga(III)-pyr-5,10,15-trispentafluorophenylcorrole complex, the emission wavelengths of such gallium(III) corroles complexes could be shifted bathochromically by up to ~3100 cm^{-1} to the near-infrared region (NIR). The described synthetic procedure establishes a facile way to obtain organic near-infrared-emitters based on gallium(III) *meso*-arylethynyl corrole complexes.

Introduction

The number of novel synthesis routes towards symmetric and asymmetric corroles has increased significantly over the past two decades. This trend was triggered by the synthesis of corroles reported by Gross, Paolesse, and Gryko *et al.*[1–4] Since then, the scope of corrole applications grew tremendously including examples in the fields of catalysis, photochemical sensors, molecular electronics, and the biomedical sector.[5–11] Due to this, the demand for tailor-made free-base and metal corrole complexes grew exponentially over the years. Various research groups performed metalation of the inner core and post-modified at the *ß*-pyrrolic and *meso*-positions of the macrocycle *via* bromination, formylation, fluoroalkylation cycloadditions,[12,13] nucleophilic aromatic substitution (S_NAr), Wittig reaction and transition metal catalyzed cross-coupling reactions.[12–22]

The aromatic substituents at the *meso*-positions of the corrole macrocycle normally twist out of planarity with respect to the 18-π-electron macrocycle and consequently, an extended π-electron conjugation to the *meso*-substituent is interrupted. Alkynyl groups as a linker between the corrole core and the aromatic systems prevent this behavior and enlarge the π-electron conjugation.

In recent years, new methodologies to synthesize π-extendend porphyrinoid macrocyclic systems were published.[19–21,24–36] Most prominently, the impressive works of Anderson et al. on the development of π-conjugated porphyrinoid oligomers, polymers, and nanorings and the fascinating methodology of Osuka et al. of synthesizing *meso*-cumulenic 2*H*-corroles from a *meso*-ethynyl-3*H*-corroles paved the way for our study to synthesize free-base and metal *meso*-aryl-ethynyl corroles.[21,29]

In the underlying work, we have synthesized free-base and gallium A_2B- and A_3-*meso*-TIPS ethynyl corroles and studied the photophysical effects of various aryl-ethynyl substituents at the *meso*-positions 5, 10, 15 of the highly fluorescent gallium A_3- and A_2B-corroles. For this purpose, an automated microreactor system was used to couple gallium A_2B- and A_3-*meso*-TIPS ethynyl corroles with the according aryliodes under *in-situ* sila-Sonogashira conditions.[37–39]

Results and Discussion

Synthesis

10-TIPS-ethynyl-5,15-(4-*t*-butylphenyl)corrole **4a**, 5,15-triiso-propylsilylethynyl-10-4-*t*-butylphenylcorrole **4b**, and 5,10,15-triisopropylsilylethynylcorrole **4c**, were synthesized according to the H_2O/methanol method of Gryko et al.[4] The HCl catalyzed condensation of 5-(4-t-butyl-phenyl)dipyrromethane **1** and TIPS-propynal **2** in H_2O/methanol and subsequent oxidation

[a] *Dr. M. Haas, D. Krisch, Dr. S. Gonglach, Dr. M. Bechmann, Prof. Dr. W. Schöfberger*
Institute of Organic Chemistry
Johannes Kepler University Linz
Altenberger Straße 69, 4040 Linz, Austria
E-mail: wolfgang.schoefberger@jku.at
https://www.jku.at/en/institute-of-organic-chemistry/team/schoefberger-lab/
[b] *Prof. Dr. M. C. Scharber*
Institute of Physical Chemistry and Linz Institute of Organic Solar Cells
Johannes Kepler University Linz
Altenberger Straße 69, 4040 Linz, Austria
[c] *M. Ertl, Prof. Dr. U. Monkowius*
Linz School of Education
Johannes Kepler University Linz
Altenberger Straße 69, 4040 Linz, Austria

Supporting information for this article is available on the WWW under https://doi.org/10.1002/ejoc.202100097

with DDQ resulted in 17% of the desired corroles **4a–c** (Scheme 1). Deprotection of the TIPS-group with TBAF led to deprotonation of the pyrrolic nitrogen atoms of the corrole macrocycles, which then degrade over time.[22,40] To circumvent this problem we decided to protect the inner core via metalation with gallium(III). Free-base corroles **4a–c** were dissolved in dry pyridine followed by addition of 4.0 equiv. of $GaCl_3$. The mixtures were heated to reflux until full consumption of the freebase corrole was obtained. The desired gallium corroles **5a–c** were obtained in 67–73% yield (Scheme 2). Following, the deprotection with TBAF in THF was carried out in quantitative yields (Scheme 2) to obtain **6a–b**, but the isolation via column chromatography was not possible due to the high reactivity of the alkyne-group with the stationary phase. To avoid degradation during purification the crude products **6a**, **6b**, and **6c** were directly used for Sonogashira cross-coupling (Scheme 3). All Sonogashira cross-coupling reactions were performed with an automated microreactor system of Vapourtec, which consists of three pumps, a mixer unit, reactor (volume = 10 mL), collector, and directly attached PC control (Figure S1). For Sonogashira cross-coupling two pumps were used, one for the catalyst system, base, and Ga-Corrole **6a**, **6b** or **6c** and the second for the corresponding aryliodide. Therefore, solution A [**6a**, **6b** or **6c**, $Pd(PPh_3)_4$ (5 mol%), CuI (8 mol%) and Hünig's base (3 equiv.) dissolved in DMF] and solution B [corresponding aryliodide (1.1–3.3 equiv.) dissolved in DMF] were mixed (solution A: flow rate 1 mL/min, V = 5 mL; solution B: 0.2 mL/min, V = 1.3 mL) and fed into the reactor (reactor volume = 10 mL, T = 80 °C, residence time = 10 min).

Full consumption of the starting Ga-corroles **6a**, **6b**, and **6c** was observed for all reactions. After filtration over Celite and purification *via* column chromatography with alumina, corroles **7a–d** were obtained in 21–63%, **8a–d** in 21–68%, and **9a–d** in 31–49% yields (Table 1). Purification using silica was not

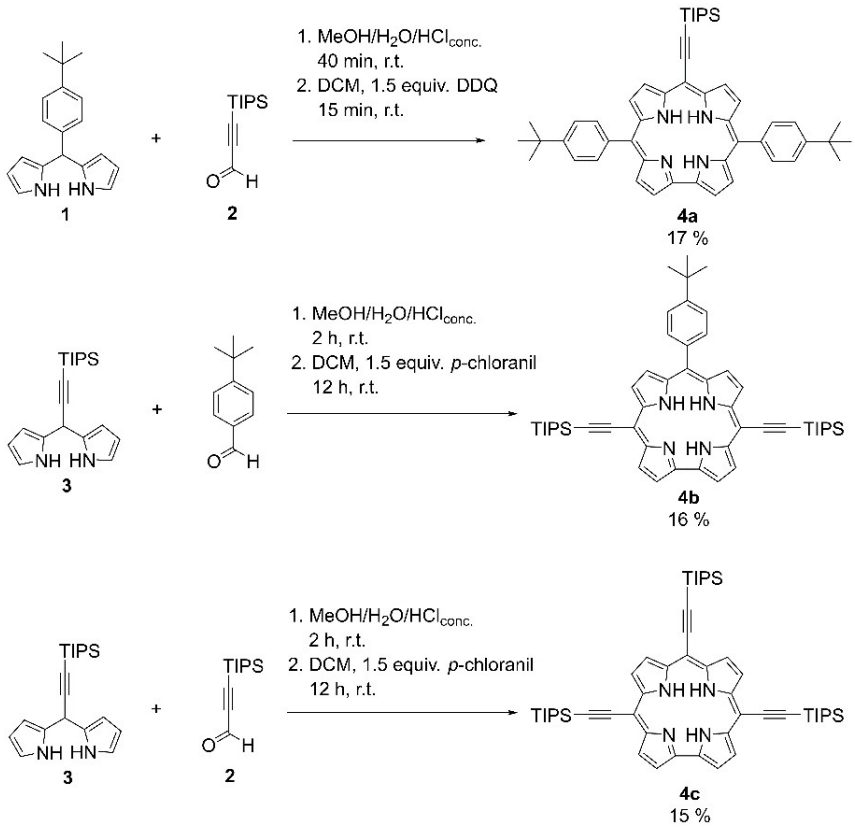

Scheme 1. Reaction scheme for the condensation of the corresponding dipyrromethane and aldehyde to the freebase corrole **4a–c**.

Table 1. Reaction yields of the Sonogashira cross-coupling with different aryliodides.

Aryliodide	one-fold Corrole	Yield (%)[a]	two-fold Corrole	Yield (%)[a]	three-fold Corrole	Yield (%)[a]
Iodobenzene	**7a**	51	**8a**	48	**9a**	31
Iodopyrene	**7b**	63	**8b**	68	**9b**	49
4-*t*-butyl-iodo-benzene	**7c**	51	**8c**	21	**9c**	n.d.
4-Iodonitro-benzene	**7d**	21	**8d**	55	**9d**	42

[a] isolated yields.

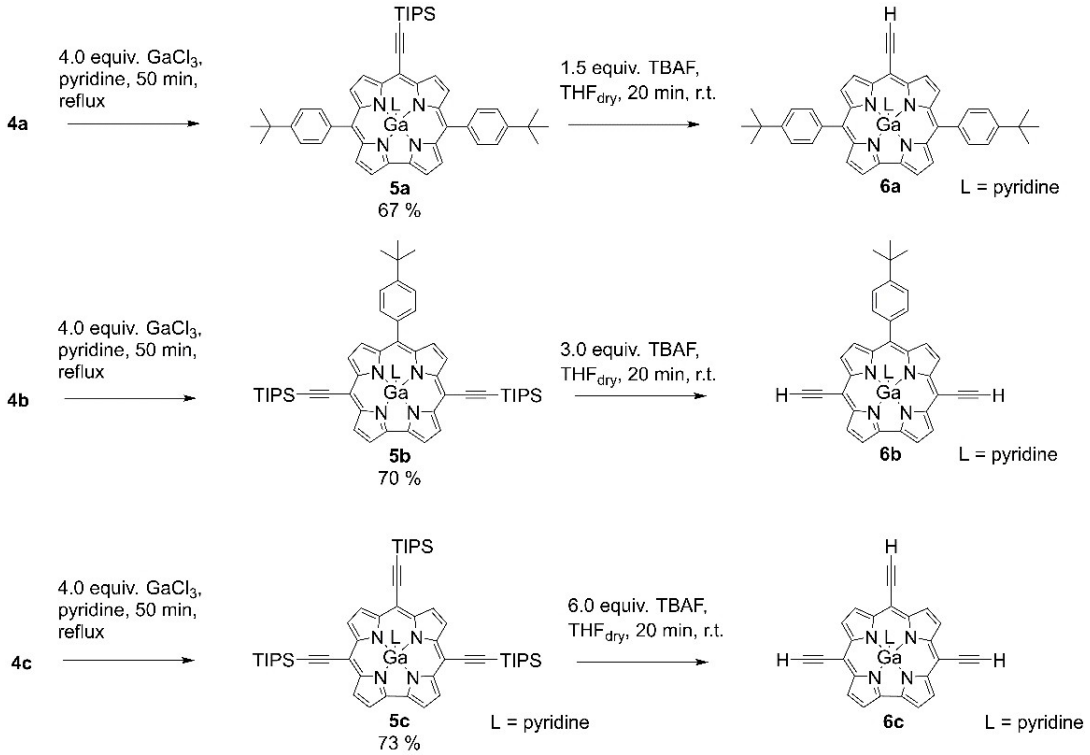

Scheme 2. Reaction scheme for the metalation of **4a–c** yielding the Ga-corroles **5a–c** and the subsequent TIPS deprotection of **5a–c** to obtain compound **6a–c**.

applicable due to the strong interaction of the products with the stationary phase, which resulted in decomposition. In Figure 1, the influence of different arylethynyl-substituents in position 10 of the corrole macrocycle on the ^{1}H-NMR chemical shifts of the *ß*-pyrrole is illustrated. Increased π-electron conjugation in **7b** exhibits a downfield shift of the highest ^{1}H-resonances (doublet, 2H, *ß*-pyrrole protons H9 and H12) to 9.65 ppm. In **7c**, a *t*-butyl-phenylethinyl substituent had no influence compared to gallium corrole **7a**. A significant upfield shift of 0.1 ppm of these *ß*-pyrrole protons was observed upon substitution with a *p*-nitro-phenyl-ethynyl group (**7d**). All other *ß*-pyrrole proton resonances of compound **7d** remain very similar in chemical shift compared to **7a**.

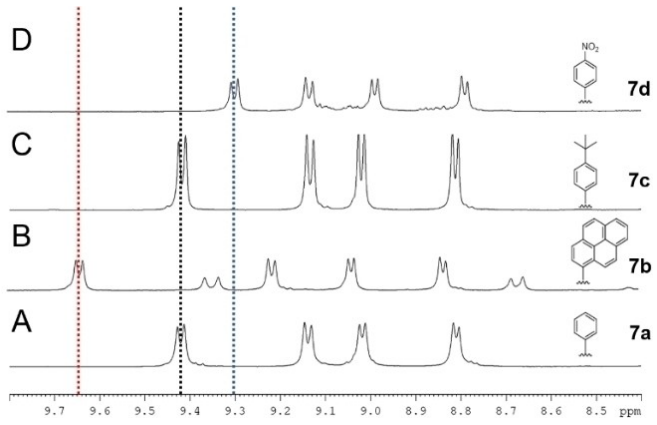

Figure 1. Stacked ^{1}H-NMR spectra showing the signals of the *ß*-pyrrole moiety of gallium corroles A) **7a**, B) **7b**, C) **7c**, and D) **7d** in $CDCl_3$.

Optical properties

Substituent effects on the optical properties of corroles **7a–d**, **8a–d**, and **9b** were investigated by UV-Vis absorption and emission spectroscopy. The UV-Vis absorptions are summarized in Table 2 and Table S1. The spectra are illustrated in Figure 2A–C. In general, the introduction of electron-donating substituents to the *para*-positions of the phenyl groups evoke a redshift of the absorption and emission maxima. Gallium corroles **5a**, **7a–d** exhibit significant substituent effects in the absorption and emission properties. Electronic absorption spectroscopy can be used to determine the magnitude of the electronic interactions between the corrole core and peripheral aryl groups. In these conjugated corroles, both the absorption and emission maxima exhibit large redshifts as compared to those of Ga(III)-*pyr*-5,10,15-trispentafluorophenylcorrole (Figure 2A, red line, Ga-*pyr*-TpFPC). Such trends are larger upon an increase in the extension of π-conjugation. As an example, Figure 3B and Figure 3C show the absorption spectra for the corroles **7b**, **8b**, **9b** which were recorded in DCM at room temperature. Their optical properties are summarized in Table S1 and Table 2. Increasing the π-electron conjugation of the corrole macrocycle by functionalization of the *meso*-positions (5-, 10- and 15-

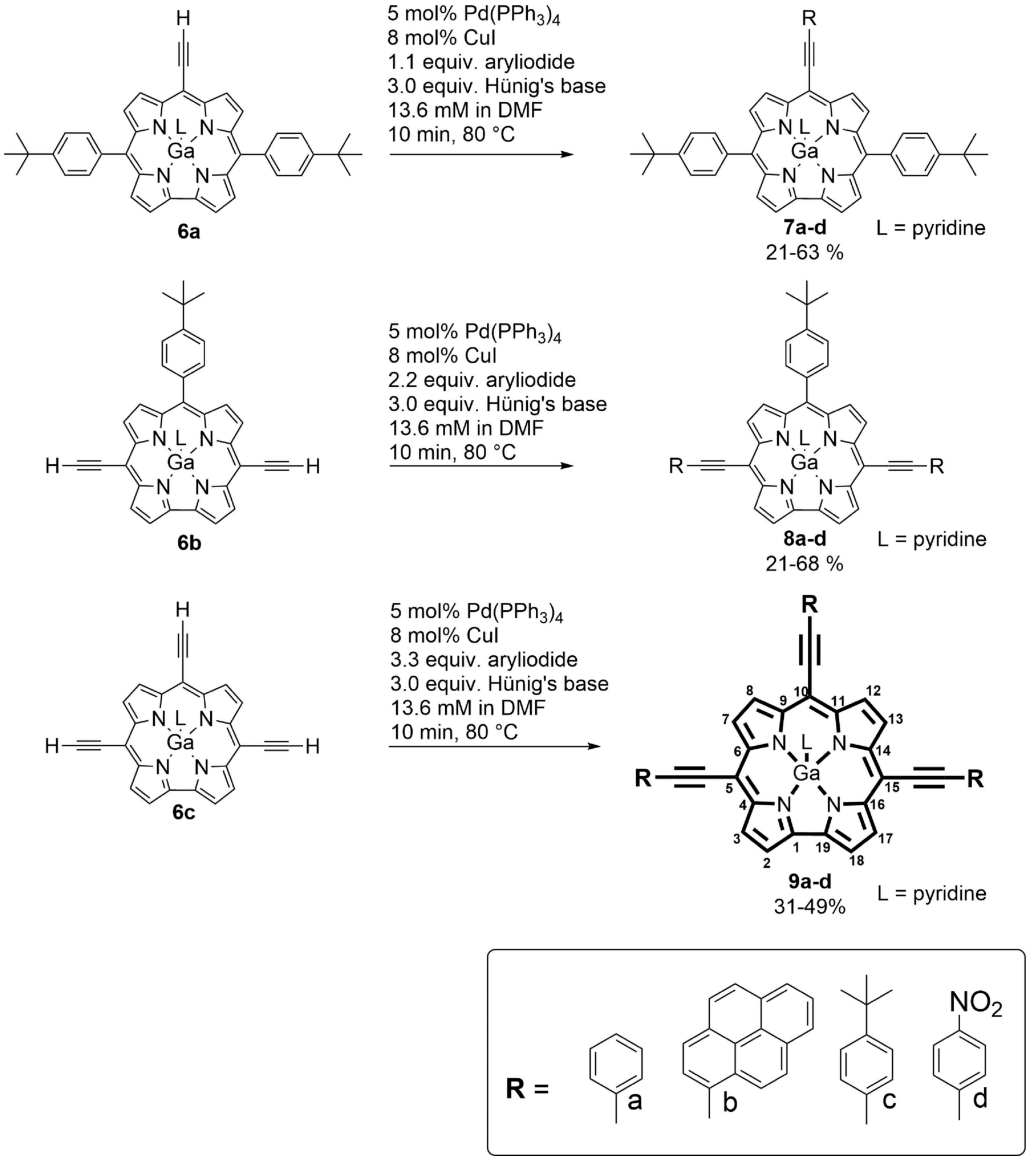

Scheme 3. Reaction scheme for the Sonogashira cross-coupling reaction of **6a–c** to obtain **7a–d**, **8a–d** and **9a–d**.

Table 2. Absorption and emission data for **4a–c**, **5a–c**, **7a–d**, **8a–d**, **9a–d**.

Complex	Soret band [nm], (ε, ×10^4)	Q-band [nm] (ε, ×10^4)	λ_{em} [a] [nm]	Φ_F [b]	τ [c] [ns]
7a	443 (5.15)	540 (4.01), 577 (3.98), 626 (4.23)	639	0.07	2.9
7b	454 (5.32), 473 (5.34)	547 (4.39), 594 (4.59), 633 (4.61)	648	0.22	3.7
7c	444 (5.32)	540 (4.07), 579 (4.04), 628 (4.35)	643	0.10	2.8
7d	425 (4.77), 458 (4.60), 493 (4.48)	576 (4.09), 617 (4.27)	615	$<$0.01	2.0
8a	446 (5.21), 470 (4.76)	560 (3.88), 612 (4.22), 664 (4.81)	676	0.26	3.7
8b	475 (5.17)	637 (4.34), 695 (4.90)	713	0.24	3.8
8c	446 (5.21), 473 (4.74)	555 (4.03), 612 (4.28), 667 (4.75)	678	0.16	3
8d	425 (4.69), 488 (4.93)	637 (4.36), 690 (4.95)	723	$<$0.01	3.9
9b	403 (3.92), 502 (4.69)	588 (3.64), 643 (3.76), 713 (4.19)	740	0.27	2.7
9d	416 (3.24), 529 (3.67)	653 (3.03), 713 (3.37)	717	$<$0.01	2.5

[a] λ_{em} represents the wavelength of the emission peak maximum ($\lambda_{exc} = \lambda_{max(Soret)}$ of the respective corrole). [b] Calculated fluorescence quantum yields were determined via the relative method employing H_2TPP (tetraphenylporphyrin) as a standard ($\Phi_F = 0.11$) in aerated toluene at an excitation wavelength of 590 nm.[41,42] [c] Experimental fluorescence lifetimes measured in aerated toluene (λ_{exc} at the respective longest emission wavelength).

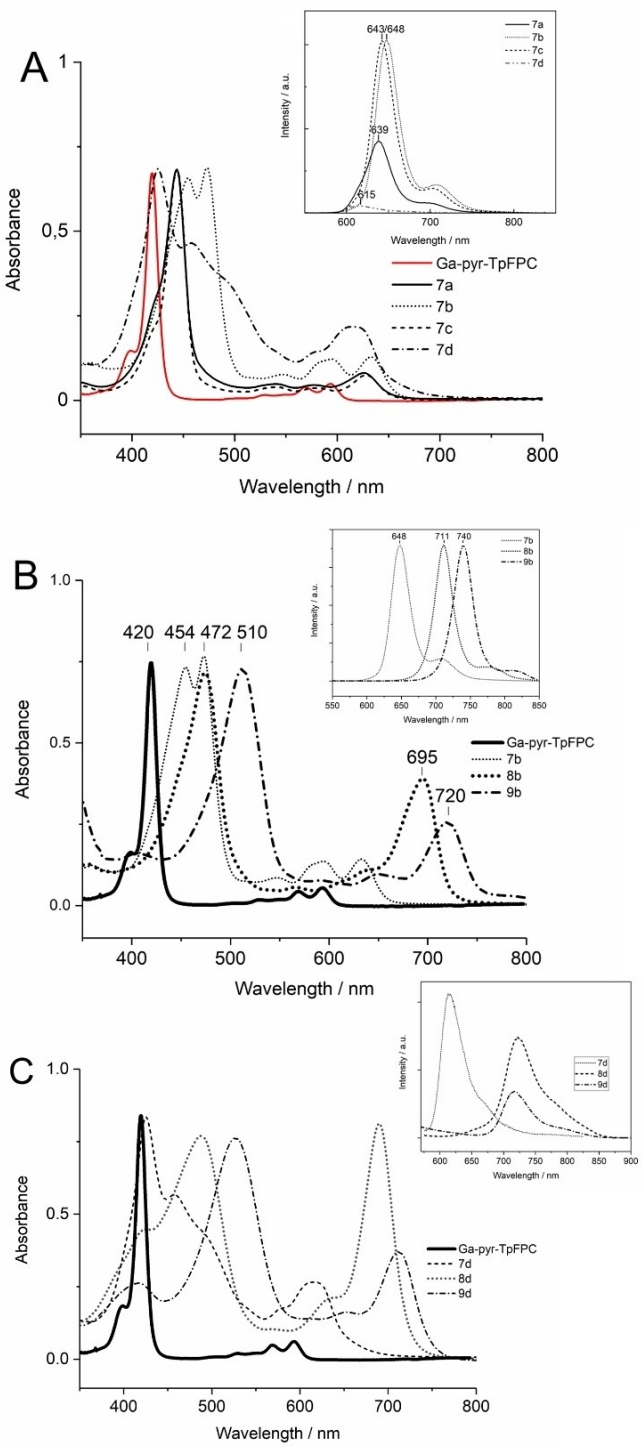

Figure 2. Substituent effects and the degree of functionalization at the *meso*-positions influences the UV-vis absorption spectra of the A_2B and A_3-gallium corroles. Normalized UV-Vis and emission spectra (inserts) of A) Ga(III)-pyr-TpFPC and one-fold functionalized **5a**, **7a**–**d** B) Ga(III)-pyr-TpFPC and one-, two, and three-fold pyrene-ethynyl functionalized corroles **7b**, **8b**, **9b** and C) Ga(III)-pyr-TpFPC and one-, two-, and three-fold nitrophenyl-ethynyl functionalized corroles **7d**, **8d**, and **9d** in DCM.

positions) with ethynylpyrene substituents produce large bathochromic shifts in both the Q and Soret (B) bands, culminating at a maximum for compound **9b** of absorption maxima at 502 (Soret band) and 713 nm (Q(I)- band, Figure 2B). These large redshifts indicate the modification of the conjugation pathway that allows effective electronic communication between the aryl moieties and the corrole core.

The relative intensities of the Q-bands change upon functionalization with the ethynylpyrene substituents; while for corrole **7b** at least three bands are clearly visible at 547, 594, and 633 nm, for **8b** and **9b** the lowest energy Q(I)-bands are significantly more intense than the Q(II)-bands and have larger extinction coefficients compared to 7a-d. The notable increase in the intensity of the lower energy Q band and the broad Soret band has been reported before for meso-arylethynyl substituted porphyrins and might originate from the loss of degeneracy of the porphyrin eg symmetry LUMO.[43–45]

Table 2 summarizes the steady-state emission data of the corroles under study. The spectra were obtained upon excitation at the λ_{max} of the Soret band and show the emission corresponding to the decay from the first excited state to two vibrational states of the ground state, Q(0,0) and Q(0,1).[46]

Consistent with the absorption spectra, emission bands of 7a-d, 8a-d, 9b,d are also red-shifted when compared to the reference spectrum of Ga-pyrTpFPC ($\lambda_{em} = 600$ nm). The fluorescence spectra of corroles **7a**–**d**, **7b**, **8b**, **9b**, and **7d**, **8d**, **9d** in Figure 2A–C (inserts) impressively illustrate the effect of *meso*-aryl-ethynyl substituents on the emission properties of these compounds. Generally, the extension of the π-conjugation shifts the emission towards lower energy. The monofunctionalized corroles of the electron-rich aryl-moieties **7a**–**c** occur at 638, 648, and 643 nm, respectively. The electron-poor system **7d** exhibits a weak emission at 615 nm, which is due to the well-known quenching effect of the attached $-NO_2$-group.[47–51] **8a** and **8c** show almost identical emission profiles possessing emission maxima at around ~677 nm. The corrole **8b** shows emission maxima at 713 nm. Again, a heavily quenched emission profile is observed for compound **8d** at 723 nm. Compound **9b** exhibits the largest shift in emission wavelength compared to Ga-pyrTpFPC and is located at 740 nm. Control measurements using degassed solutions under argon revealed no sensitivity of the observed fluorescence intensity to the presence of oxygen. The emission lifetimes of all compounds are found to be 2.0–3.9 ns, which is in the expected range for fluorescence.

The excitation spectra recorded at the wavelength of maximum emission nicely resembles the absorption spectra of each corrole.

Theoretical Studies

To rationalize the effects of introducing the aryl-ethynyl groups at the *meso*-positions of the corrole macrocycles, the structural, electronic, and optical properties of **7a**–**d**, **8a**–**d**, **9a**–**d** were theoretically investigated using DFT and TDDFT methods.

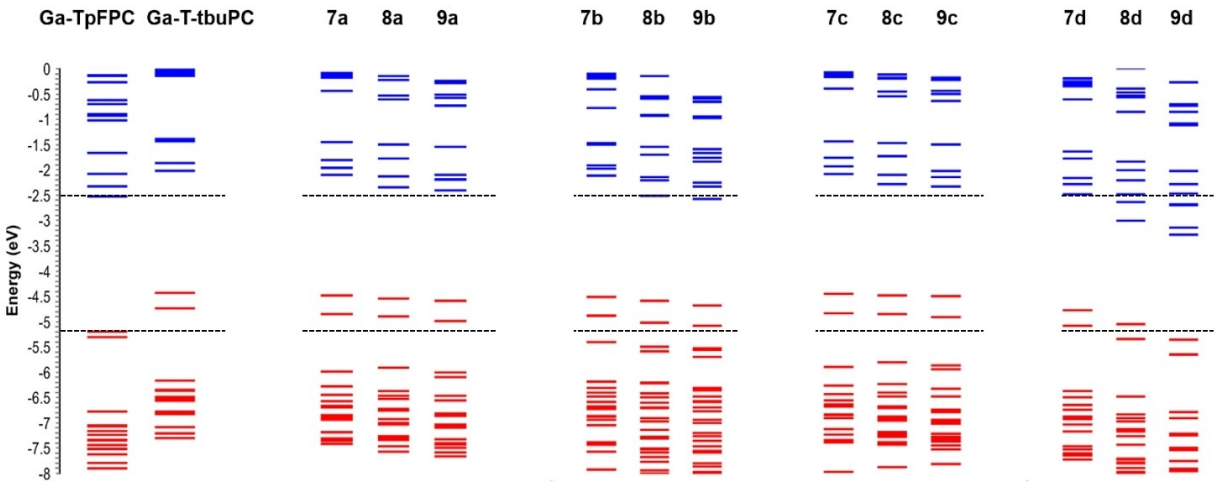

Figure 3. Calculated energy level diagrams for **Ga(-pyr)-TpFPC**, **Ga(-pyr)-*t* bu-PC**, **7a–d**, **8a–d**, **9a–d**. Dashed horizontal lines denote the $\Delta E_{HOMO-LUMO}$-gap of reference **Ga(-pyr)-TpFPC**.

(a) Molecular Structures

Meso-aryl gallium A_3-corroles are known to possess a slight dome-shaped structure of the macrocycles with almost perpendicular phenyl groups, and our calculations confirm this, with each phenyl group found to be at an angle of approximately $75° \pm 1°$ with respect to the aromatic plane. This is in stark contrast to the newly synthesized gallium corroles **7a–d**, **8a–d**, and **9b**. The geometry optimized structures show that the aryl-moieties attached at the linear ethynyl-groups are orientated coplanarly to the macrocycle ring system. As a result, strong electronic communication between the macrocycle and the *meso*-substituents can be expected. The valence orbital energies and the calculated electronic absorption spectra of these main group metal corrole are qualitatively similar to those of a metalloporphyrin, e.g. zinc porphyrins. The "four-orbital model" holds well also for corroles. The a_2 and b_1 HOMOs of the gallium corroles are rough analogues of the well-known a1u and a2u porphyrin HOMOs, respectively. Thus, as in the case of porphyrins, there are two nearly equi-energetic π-cation radical states for corroles. The nuclear geometries were optimized using DFT, and TDDFT was used to generate the vertical excitation energies at the fixed nuclear ground state geometry, as well as the relaxed S_1 geometry.

(b) Ground-State Electronic Structure and Optical Spectra

To provide an explanation of the UV/vis spectral changes accompanying the substitution of the *meso*-position with aryl-ethynyl groups, TDDFT calculations of the electronic absorption spectra in dichloromethane solution were performed for **7a–d**, **8a–d**, **9a–d**. Before dealing with the excited states, we briefly discuss the ground-state electronic structure of the investigated metal corroles. To highlight the electronic effects of the different substituents, the electronic structure of the known gallium corroles Ga(-pyr)-TpFPC and Ga(-pyr)-*t*-bu-PC are taken as a reference. An energy level scheme of the highest occupied (red) and lowest unoccupied (blue) Kohn-Sham orbitals of **Ga(-pyr)-TpFPC** and **Ga(-pyr)-*t*-bu-PC** and **7a–d**, **8a–d**, and **9a–d** are shown in Figure 3.

The plots of the highest occupied and of the lowest unoccupied MOs of these compounds are displayed in Figure 4A–C. As shown by Hush and co-workers and later by Gosh. the Gouterman four-orbital model of porphyrins can also be employed for corrole systems.[52,53] However if the corrole C_{2v} symmetry is enforced the D_{4h} symmetric porphyrin a_{1u}, a_{2u} HOMOs, become a_2 and b_1, and the e_g LUMOS become a_2 and b_1. Transitions between these four states will give rise to four excited states, of which two are $^1A_1$ and two are $^1B_2$. Mixing of the occupied orbitals a_1 and b_2 will change the energies of the transitions to these excited states and two pairs of transitions each will separate into the B (Soret) and Q band. The relative intensity of these bands is governed by the oscillator strength of the respective vertical transitions to the $^1A_1$, $^1B_2$ excited states. Overall, the transitions to the low-energy, Q band are less intense than those to the B band, but band intensity increases with a decrease of the degeneracy of the a_2 and b_1 HOMO and LUMO orbital pairs. In our pyridine-corrole gallium complexes, the unoccupied pyridine orbital of b_2 symmetry is energetically close or even overlaps with the two a_2 and b_1 Gouterman LUMOs. This leads to mixed transitions from Gouterman HOMOs to Gouterman LUMOs and the low-lying pyridine b_2 LUMO. Substituting the corrole in a pyridine-corrole gallium complex with arylic groups, has the potential to extend the electron delocalization of the Gouterman frontier-orbitals by conjugation between the corrole and aryl π systems and hence change their relative energies and ultimately cause changes in the absorption spectra. Following the substitution, we expect the following canonical effects: (i) Substitution of electron-donating groups adds more electrons to the corrole system and thus increases electron-electron repulsion (or decreases the effective nuclear charge) and HOMO and LUMO energies increase. (ii) electron-withdrawing groups remove electrons and, thus

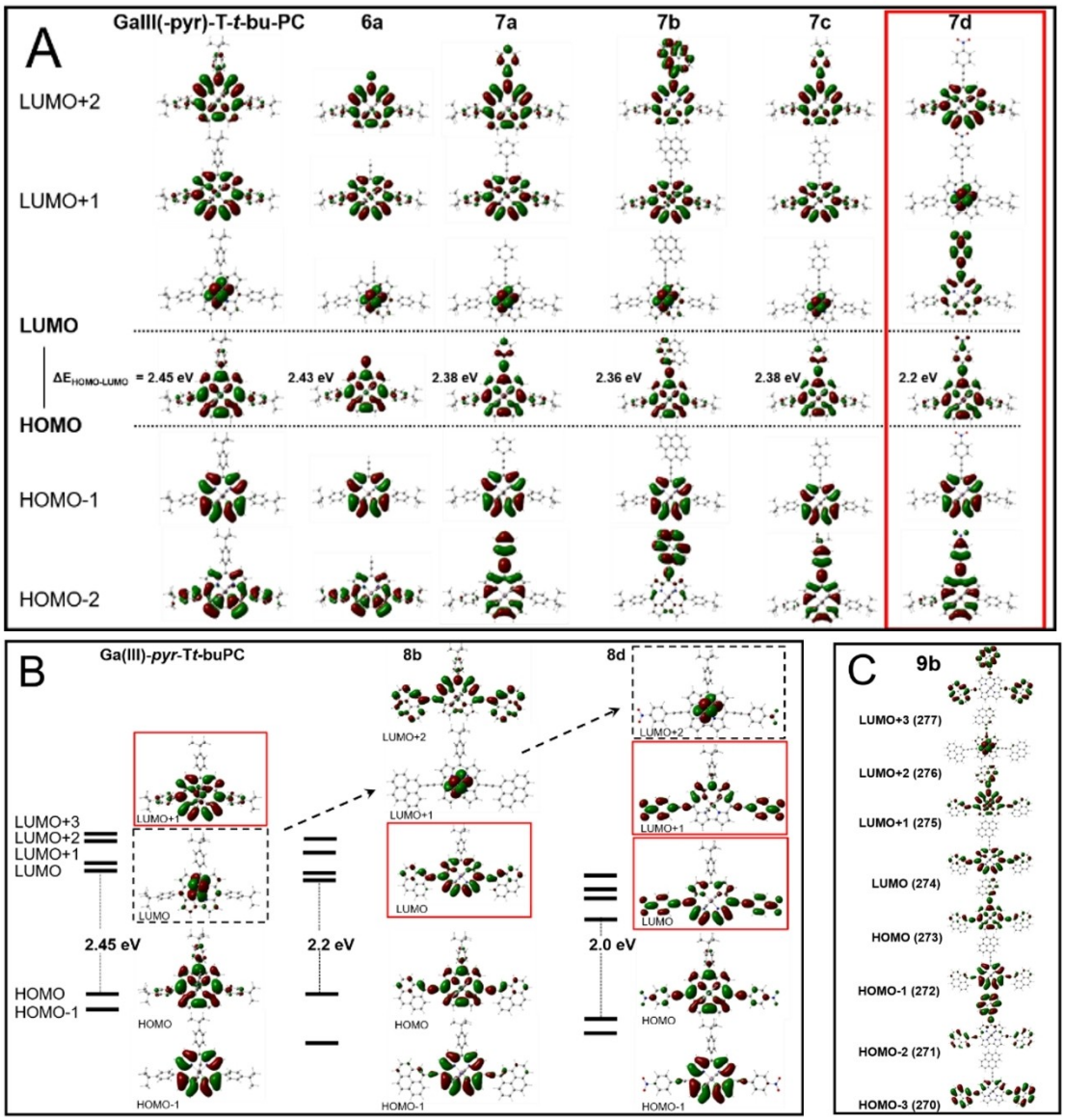

Figure 4. Plots of the frontier orbitals of A) **6a**, **7a**–**d**, B) **Ga(III)-pyr-T-t-bu-PC**, **8c**, **8d**, C) **9b** after geometry optimization,

decreases the HOMO and LUMO energies (iii) electron-donating groups usually act through an occupied orbital. It must be energetically close to the HOMO and therefore, it has a stronger effect on the HOMO than on the LUMO. (iv) electron-withdrawing groups act through a virtual (unoccupied) orbital, which interacts more strongly with the LUMO. As a consequence, electron-donating and withdrawing groups are both expected to lower the HOMO-LUMO gap in organic molecules. The two HOMOs, a_2 and b_1, are near-degenerate, as are the two LUMOs, a_2 and b_1. In the case of Ga-pyr-t-bu-PC these four frontier orbitals are well-separated energetically from the rest of the orbital energy spectrum. In comparison to this, in gallium corroles **7**–**9** higher-lying orbitals shift down in energy due to the π-conjugation of aryl-groups via the ethynyl-groups to the macrocyclic system.The HOMO-1 and HOMO of **7a**–**c** resemble the HOMO-1(a_1) and HOMO(b_1) of Ga(-pyr)-TpFPC and Ga(-pyr)-*t*-bu-PC (C_{2v} symmetry). The LUMO and LUMO+1 of **7a**–**c** match also well with the LUMO and LUMO+1 of Ga(-pyr)-TpFPC and Ga(-pyr)-*t*-bu-PC (C_{2v} symmetry). In the nitro derivatives and in the parent Ga(-pyr)-TpFPC and Ga(-pyr)-*t*-bu-PC, a fairly large energy gap separates the HOMO-1 from the lower-lying MOs, which are largely localized on the aryl groups and on the pyrrolenine ring. Compared to gallium aryl ethynyl corroles **7a**, **c**, **8a**, **c**, **9a**, **c**, the nitro derivatives (**7d**, **8d**, **9d**) and the pyrenyl derivatives (**8b**, **9b**) interpose the LUMO with π-nitro-phenyl-ethynyl and π-pyrenyl-ethynyl orbitals (Figure 4A–C). According to the level scheme of Figure 3, the outstanding effect of introducing nitro groups into the gallium corroles is the stabilization of the frontier MOs (HOMO, HOMO-1, HOMO-2, LUMO, LUMO+1, LUMO+2, etc.). Additionally, in comparison to the reference Ga(-pyr)-*t*-bu-PC corrole, a splitting of the LUMO states occurs. We discuss now how the previously

discussed electronic structure changes accompanying the coupling of the aryl-ethynyl moieties to the corrole macrocycle reflect on the UV-visible spectroscopic properties of the investigated corroles.

The excitation energies and oscillator strengths calculated for the lowest singlet excited states of the parent GaTpFPC and the derivative **9b** are reported in Figure 5A, B together with the major one-electron transitions contributing to the excited-state solution vectors. The positions and oscillator strengths of the calculated Soret- and Q-band transitions of **9b** and GaTpFPC are well comparable to the experimentally observed ones illustrated in Figure 2B. Inspection of the computed optical transitions of compound **9b** exhibits that the most intense Soret-band transition occurs from HOMO-1(MO272)→LUMO+1(MO275) at 500 nm (Figure 5A). This stands in stark contrast to the Soret-band transitions observed for GaTpFPC, where transitions at 420 nm occur from different frontier molecular orbitals occur (HOMO-1(218) and HOMO (219)→LUMO (220) and LUMO+1 (221)) (Figure 5B). Figure 6 illustrates TD-DFT spectra of **9b** at different torsion angles (C_α–C_m–C_i–C_o = 0°, 45°, 90°) of the attached pyrenyl moieties with respect to the macrocyclic ring system. A 90° rotation of all *meso*-pyrenyl groups exhibits a strong hypsochromic shift and the Soret band maximum is at 420 nm. This corresponds well to UV-vis absorption spectra observed for regular *meso*-substituted corrole derivatives.

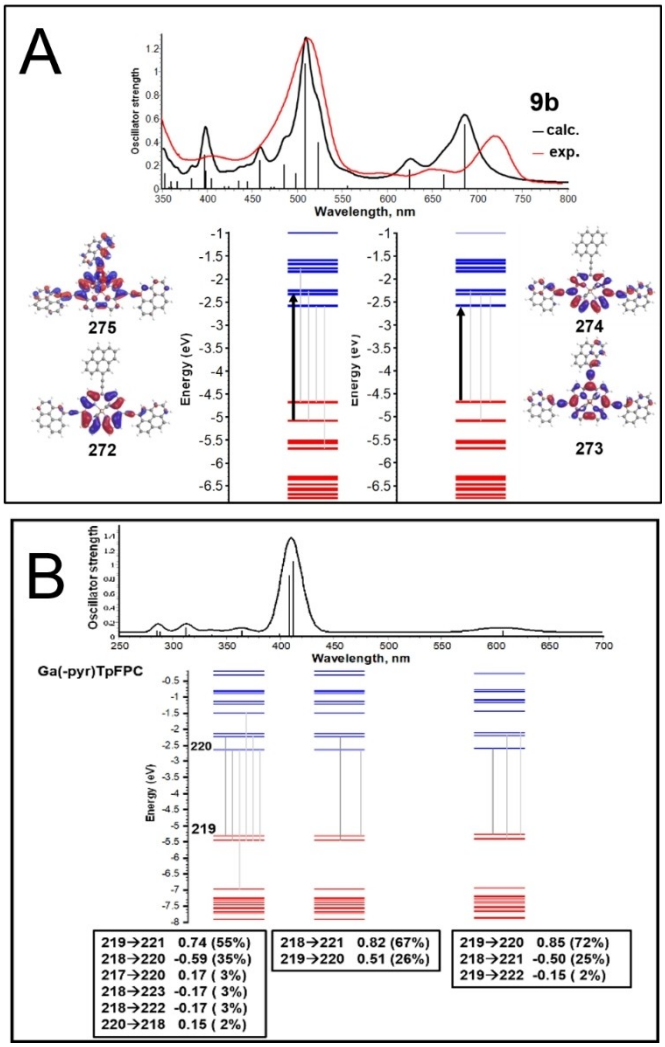

Figure 5. Composition, vertical excitation energies, E (eV/nm), and oscillator strengths, for the lowest optically allowed excited states of A) **9b** and B) **Ga(-pyr)TpFPC** in CH_2Cl_2.

Conclusion

To conclude, we have presented the synthesis of gallium(III) A_2B- and A_3-*meso*-arylethynyl corrole complexes and have studied the optical properties of different aryl substituents by means of photophysical experiments and DFT-calculations. Electronic absorption spectroscopy can be used to determine the extent of the electronic interactions between the corrole core and peripheral aryl groups. In these π-conjugated corroles, both the absorption and emission maxima exhibit large red-shifts as compared to those of the well-known Ga(III)-*pyr*-5,10,15-trispentafluorophenylcorroles. Such trends are larger upon increasing the extension of π-conjugation. The novel gallium(III)-pyridine-5,10,15-pyrenylethynyl-corrole complex **9b**

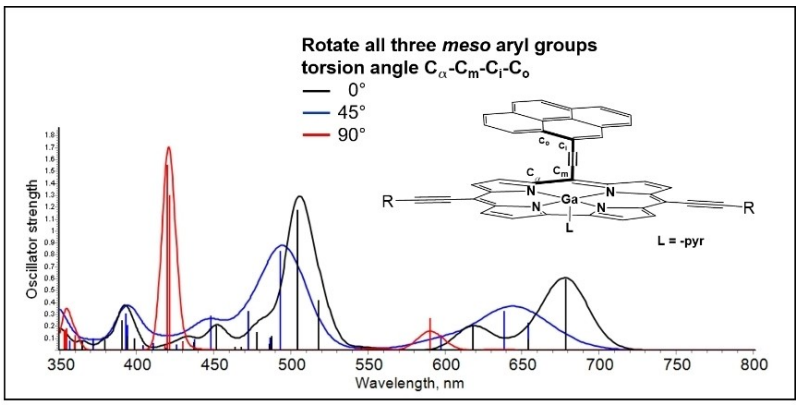

Figure 6. TD-DFT spectra of **9b** at different torsion angles (C_a–C_m–C_i–C_o = 0°, 45°, 90°) of the attached pyrenyl groups.

exhibits a Soret-band maximum at 510 nm and emission maximum at 740 nm with fluorescence quantum yields $\Phi_F =$ 0.27 in aerated toluene. The electron-poor A_2B- and A_3- gallium (III)-pyridine-4-nitrophenyl-ethynyl)-corrole complexes **7d**–**9d** exhibit quenched emission. The quenching effect originates from the attached $-NO_2$-group. Our ongoing work focuses on converting the presented metal TIPS-ethynyl-corrole precursors to corrole dimers, oligomers, and polymers. Moreover, we now aim in our laboratory to synthesize novel corrole nanorings following the examples done for the extensively explored porphyrin analogs. These homo- or bimetallic corrole assemblies could provide a framework for its incorporation as light-harvesting-catalyst assemblies.

Experimental Section

Materials and methods

All chemicals were purchased from Alfa Aesar, Fluka, Merck, or Sigma-Aldrich and were used without further purification. 5-(4-t-butylphenyl)dipyrromethane **1**, 3-triisopropylsilylpropynal **2**, 5-triisopropyl-ethynyldipyrromethane **3**, gallium(III) pyridine-5,10,15-trispentafluoro-phenylcorrole (GaTpFPC) were synthesized according to literature procedures.[54,53,23] DCM stored over molar sieve MB-SPS-7 using an M. Braun Inert gas-System GmbH (Garching, Germany) under argon atmosphere. All NMR solvents were purchased from Euriso-Top. TLC was performed on Macherey-Nagel silica gel 60 (0.20 mm) with fluorescent indicator UV254 on aluminium plates and on Merck aluminium oxide 60 (0.20 mm) with fluorescent indicator UV254 on aluminium plates. For chromatography, silica-gel columns were prepared with silica-gel 60 (0.070–0.20 mesh) from Grace and aluminium oxide 60, basic, activity level II from Acros. Proton and carbon NMR spectra were recorded on a Bruker AvanceIII 700 MHz spectrometer and on a Bruker AvanceIII 300 MHz NMR spectrometer. The chemical shifts are given in parts per million (ppm) on the delta scale (δ) and are referred to the used deuterated solvent for ^{1}H-NMR and to TFA for ^{19}F-NMR. High-resolution mass spectra were obtained using an Agilent 6520 Q-TOF mass spectrometer with an ESI source and an Agilent G1607 A coaxial sprayer or a Thermo Fisher Scientific LTQ Orbitrap XL with an Ion Max API Source. UV-Vis absorption spectra were collected on a Varian CARY 300 Bio spectrophotometer from 200 to 900 nm. Fluoresence lifetimes were determined with a SPC-130 (Becker&-Hickl) time-correlated single-photon counting set-up equipped with a 405 nm PicoQuant nanosecond laser.

Synthesis procedures

Synthesis of 5,15-4-t-butylphenyl-10-triisopropylsilylethynyl-corrole (4a): 5-(4-t-butylphenyl)dipyrromethane **1** (500 mg, 1.80 mol) and TIPS-propynal **2** (219 µL, 0.90 mmol) were dissolved in MeOH (94 mL). H_2O (94 mL) and $HCl_{conc.}$ (5.2 mL, 36%) were added and the solution was stirred for 40 min at room temperature. The mixture was extracted thrice with DCM, the organic phase was dried over Na_2SO_4 and concentrated. The crude product was diluted with DCM (400 mL), DDQ (306 mg, 1.35 mmol) added and stirred for 15 min at room temperature. Subsequent evaporation to dryness and purification *via* column chromatography (silica, DCM/heptane [1:1]) afforded the product **4a** as a green solid (113 mg, 17%). $R_f = 0.65$ (DCM/heptane (1:1); ^{1}H-NMR (500 MHz, $CDCl_3$, 25 °C): $\delta = 9.23$–7.77 (m, 16 H, pyrrole-H + phenyl-H), 1.62 (s, 21 H, –TIPS), 1.48 (s, 18 H, $-CH_3$); HRMS *m/z*: calcd. for $C_{42}H_{41}N_4Si^-$: 741.4358; found 741.4325 $[M-H]^-$; λ_{max} nm (log ε): 294 (4.03), 430 (5.08), 578 (4.09), 598 (4.12), 627 (4.11), 663 (3.59); Emission $\lambda_{max} =$ 680 nm.

Synthesis of 5,15-Triisopropylsilylethynyl-10-4-t-butylphenyl-corrole (4b): 4-t-butylbenzaldehyde (230 µL, 1.37 mmol) and **2** (897 mg, 2.75 mol) were dissolved in MeOH (144 mL). H_2O (136 mL) and $HCl_{conc.}$ (8 mL, 36%) were added and the solution was stirred for 2 h at room temperature. The mixture was extracted thrice with DCM, the organic phase was dried over Na_2SO_4 and concentrated. The crude bilane was diluted with DCM (620 mL) and *p*-chloranil (507 mg, 2.06 mmol) added. The solution was stirred overnight and then evaporated to dryness. Subsequent purification *via* column chromatography (silica, DCM/heptane [1:1]) afforded the product **4b** as a green solid (170 mg, 16%). ^{1}H-NMR (300 MHz, $CDCl_3$, 25 °C): $\delta = 9.28$ (s, 2 H, pyrrole-H), 8.90 (s, 4 H, pyrrole-H), 8.63 (s, 2 H, pyrrole-H), 8.09 (s, 2 H, phenyl-H), 7.78 (s, 2 H, phenyl-H), 1.63 (s, 9 H, $-CH_3$), 1.46 (s, 42 H, –TIPS); *m/z*: calcd. for $C_{57}H_{61}N_4Si_2^-$: 789.4753; found 789.2 $[M-H]^-$; UV-Vis (DCM, nm) λmax: 421, 433, 464, 607, 648, 684; Emission $\lambda_{max} = 700$ nm.

Synthesis of 5,10,15-triisopropylsilylethynylcorrole (4c): TIPS-Propynal (124 µL, 0.51 mmol) and **2** (333 mg, 1.02 mol) were dissolved in MeOH (54 mL). H_2O (54 mL) and $HCl_{conc.}$ (3 mL, 36%) were added and the solution was stirred for 2 h at room temperature. The mixture was extracted thrice with DCM, the organic phase was dried over Na_2SO_4 and concentrated. The crude product was diluted with DCM (340 mL), *p*-chloranil (188 mg, 0.76 mmol) added and stirred overnight at room temperature. Subsequent evaporation to dryness and purification *via* column chromatography (silica, DCM/heptane [1:1]) afforded the product **4c** as a green solid (65 mg, 15%). $R_f = 0.93$ (DCM/heptane (1:1); ^{1}H-NMR (700 MHz, $CDCl_3$, 25 °C): δ_H, ppm 9.26 (s, 4 H, pyrrole-H), 8.82 (s, 4 H, pyrrole-H), 1.44–1.48 (m, 63 H, -TIPS); ^{13}C-NMR (175 MHz, $CDCl_3$, 25 °C): δ_C, ppm 145.9, 137.1, 130.2, 128.7, 127.8, 122.1, 116.7, 106.9, 100.6, 97.7, 95.3, 30.9, 20.2, 20.1, 12.9, 12.8; HRMS *m/z*: calcd. for $C_{52}H_{74}N_4Si_3$–H^+: 837.5149 $[M-H]^-$; found 837.5151; UV-vis (CH_2Cl_2): λ_{max}, nm (log ε): 421 (4.99), 441 (5.34), 470 (5.06), 580 (4.36), 607 (4.55), 621 (4.62), 660 (4.66), 685 (4.26), 770 (4.22); Emission $\lambda_{max} =$ 670, 705, 788 nm.

General procedure for the gallium metalation: The corresponding freebase corrole was dissolved in pyridine (4.2 mM) and flushed with argon. Subsequently, $GaCl_3$ (4.0 equiv.) was added and the reaction was refluxed under argon until full consumption of the starting material. Afterward, the reaction mixture was concentrated under vacuum and purified *via* column chromatography.

Synthesis of Gallium(III)-pyridine-5,15-4-t-butylphenyl-10-triisopropylsilylethynylcorrole (5a): Freebase corrole **4a** was metalated according to the general procedure for the gallium metalation. Purification was accomplished *via* column chromatography (silica, DCM + 1% pyridine) and the product **5a** was obtained as a green solid (360 mg, 67%). ^{1}H-NMR (500 MHz, $CDCl_3$, 25 °C): $\delta = 9.35$ (d, J(H,H) = 4.5 Hz, 2 H, pyrrole-H), 9.10 (d, J(H,H) = 4.5 Hz, 2 H, pyrrole-H), 9.00 (d, J(H,H) = 3.8 Hz, 2 H, pyrrole-H), 8.80 (d, J(H,H) = 3.8 Hz, 2 H, pyrrole-H), 8.24 (d, J(H,H) = 7.9, 4 H, phenyl-H), 7.81 (d, J(H,H) = 8.3, 4 H, phenyl-H), 6.66 (t, J(H,H) = 7.7 Hz, 1 H, pyridine-H), 5.87–5.90 (m, 2 H, pyridine-H), 3.21 (d, J(H,H) = 5.2 Hz, 2 H, pyridine-H), 1.63 (s, 18 H, CH_3), 1.44–1.45 (m, 21 H, TIPS); ^{13}C-NMR (125 MHz, $CDCl_3$, 25 °C): $\delta = 149.9$, 147.7, 142.4, 140.6, 138.8, 138.3, 137.4, 135.5, 134.3, 129.5, 125.9, 125.9, 124.4, 123.9, 123.4, 118.6, 115.4, 109.9, 93.4, 88.2, 34.8, 31.7, 19.2, 12.0; HRMS *m/z*: calcd. for $C_{55}H_{60}GaN_5Si$: 887.3874 [*M*]; found [M−H] 887.3881; λ_{max} nm (log ε): 255 (3.95), 296 (4.01), 347 (3.61), 415 (4.45), 438 (5.13), 524 (3.60), 539 (3.70), 577 (3.66), 625 (4.14); Emission $\lambda_{max} = 636$, 699 nm.

Synthesis of Gallium(III)-pyridine-5,15-Triisopropylsilyl-ethynyl-10-4-*t*-butylphenylcorrole (5 b): Freebase corrole **4 b** was metalated according to the general procedure for the gallium metalation. Purification was accomplished *via* column chromatography (silica, DCM + 1 % pyridine) and the product **5 b** was obtained as a green solid (563 mg, 70 %). ^{1}H-NMR (300 MHz, CDCl3, 25 °C): δ = 9.55 (d, J(H,H) = 4.6 Hz, 2 H, pyrrole-H), 9.31 (d, J(H,H) = 3.9 Hz, 2 H, pyrrole-H), 9.15 (d, J(H,H) = 4.0 Hz, 2 H, pyrrole-H), 8.83 (d, J(H,H) = 4.3 Hz, 2 H, pyrrole-H), 8.08 (d, J(H,H) = 7.8 Hz, 2 H, phenyl-H), 7.76 (d, J(H,H) = 8.3 Hz, 2 H, phenyl-H), 6.71 (t, J(H,H) = 7.8 Hz, 1 H, pyridine-H), 6.00–5.95 (m, 2 H, pyridine-H), 3.54–3.52 (m, 2 H, pyridine-H), 1.62 (s, 3 H, –CH_3), 1.47–1.46 (m, 42 H, TIPS); ^{13}C-NMR (75 MHz, $CDCl_3$, 25 °C): δ = 149.9, 145.0, 143.6, 142.9, 140.1, 138.8, 138.6, 135.1, 134.1, 126.9, 126.0, 124.6, 124.0, 123.9, 116.9, 113.3, 108.6, 96.1, 95.2, 34.8, 31.7, 29.7, 19.1, 11.9; HRMS *m/z*: calcd. for $C_{52}H_{63}GaN_4O_2Si_2^-$: 901.3824 [*M*-pyridine + COOH]; found 901.3816; UV-Vis (DCM, nm) λ_{max} = 255 (3.95), 296 (4.01), 347 (3.61), 415 (4.45), 438 (5.13), 524 (3.60), 539 (3.70), 577 (3.66), 625 (4.14); Emission λ_{max} = 652, 718 nm.

Synthesis of Gallium(III)-pyridine-5,10,15-Triisopropyl-silylethynyl-corrole (5 c): Freebase corrole **4 c** was metalated according to the genereal procedure for the gallium metalation. Purification was accomplished *via* column chromatography (silica, DCM + 3 % pyridine) and the product **5 c** was obtained as a green solid (122 mg, 73 %). ^{1}H-NMR (300 MHz, $CDCl_3$, 25 °C): δ = 9.54 (d, J(H,H) = 4.8 Hz, 2 H, pyrrole-H), 9.38 (d, J(H,H) = 3.8 Hz, 2 H, pyrrole-H), 9.23 (d, J(H,H) = 4.0 Hz, 2 H, pyrrole-H), 9.04 (d, J(H,H) = 4.0 Hz, 2 H, pyrrole-H), 6.73–6.68 (m, 1 H, pyridine-H), 5.96–5.91 (m, 2 H, pyridine-H), 3.17–3.16 (m, 2 H, pyridine-H),1.47–1.46 (m, 63 H, TIPS); ^{13}C-NMR (75 MHz, $CDCl_3$, 25 °C): δ = 146.3, 144.4, 142.4, 139.9, 139.1, 135.7, 127.7, 125.2, 124.5, 124.1, 116.9, 108.8, 108.0, 97.2, 96.9, 95.1, 92.2, 19.2, 19.1, 12.0, 11.9; UV-Vis (DCM, nm) λ_{max} = 456, 466, 567, 609, 659; Emission λ_{max} = 664, 732 nm.

General procedure for the deprotection: The corresponding Gallium corrole (1 equiv.) was dissolved in THF (11 mM) and purged with argon followed by the addition of 1 M TBAF in THF. The solution was allowed to stir under argon until complete consumption of the starting material, followed by concentration under vacuum.

Synthesis of Gallium(III)-pyridine-5,15-4-t-butylphenyl-10-ethynyl-corrole (6 a): Gallium corrole **5 a** was deprotected according to the general procedure for the deprotection utilizing 1.5 equiv. TBAF. The product was directly used for the next reactions without further purification.

Synthesis of Gallium(III)-pyridine-5,15-ethynyl-10-4-t-butyl-phenylcorrole (6 b): Gallium corrole **5 b** was deprotected according to the general procedure for the deprotection utilizing 3.0 equiv. TBAF. The product was directly used for the next reactions without further purification.

Synthesis of Gallium(III)-pyridine-5,10,15-ethynylcorrole (6 c): Gallium corrole **5 c** was deprotected according to the general procedure for the deprotection utilizing 6.0 equiv. TBAF. The product was directly used for the next reactions without further purification.

General procedure for the one-fold Sonogashira cross-coupling reaction in the flow-reactor: Solution A [**6 a** (0.405 mmol), $Pd(PPh_3)_4$ (27 mg, 5 mol%), CuI (7 mg, 8 mol%) and Hünig's base (238 µL, 3 equiv.) dissolved in 30 mL DMF] and solution B [corresponding aryliodide (2.2 equiv.) dissolved in 2.6 mL DMF] were mixed (solution A: flow rate 1 mL/min, V = 5 mL; solution B: 0.2 mL/min, V = 1.3 mL) and fed into the reactor (reactor volume = 10 mL, T = 80 °C, residence time = 10 min). The collected product was filtered through Celite with EtOAc as solvent, followed by concentration under vacuum.

Synthesis of Gallium(III)-pyridine-5,15-4-t-butylphenyl-10-phenylethynylcorrole (7 a): Gallium corrole **6 a** was cross-coupled, according to the general procedure for the Sonogashira cross-coupling reaction utilizing 1.1 equiv. iodobenzene. Purification was accomplished *via* column chromatography (aluminiumoxide 60, basic, acitivity level II, DCM + 1 % pyridine) and the product **7 a** was obtained as a green solid (28 mg, 51 %). ^{1}H-NMR (300 MHz, $CDCl_3$, 25 °C): δ = 9.41 (d, J(H,H) = 4.4 Hz, 2 H, pyrrole-H), 9.12 (d, J(H,H) = 4.4 Hz, 2 H, pyrrole-H), 9.01 (d, J(H,H) = 3.8 Hz, 2 H, pyrrole-H), 8.80 (d, J(H,H) = 3.8 Hz, 2 H, pyrrole-H), 8.26 (d, J(H,H) = 7.95 Hz, 4 H, phenyl-H), 7.98 (d, J(H,H) = 7.43 Hz, 2 H, phenyl-H), 7.83 (d, J(H,H) = 7.99 Hz, 4 H, phenyl-H), 7.50–7.55 (m, 2 H, phenyl-H), 7.38–7.44 (m, 1 H, phenyl-H), 6.83 (t, J(H,H) = 7.17 Hz, 1 H, pyridine-H), 6.13–6.17 (m, 2 H, pyridine-H), 4.40 (s, 2 H, pyridine-H), 1.63 (s, 18 H, CH_3); ^{13}C-NMR (75 MHz, $CDCl_3$, 25 °C): δ = 150.0, 147.1, 144.3, 140.5, 138.3, 138.0, 137.6, 135.6, 134.3, 131.2, 129.4, 128.5, 127.4, 126.1, 125.2, 124.5, 123.8, 123.2, 118.7, 115.5, 93.5, 92.8, 87.7, 34.9, 31.7; HRMS *m/z*: calcd. for $C_{56}H_{43}GaN_5^-$: 806.2780 [*M*–H]$^-$; found 805.2633; λ_{max} nm (log ε): 292 (4.30), 443 (5.15), 540 (4.01), 577 (3.98), 626 (4.23); Emission λ_{max} = 638 nm.

Synthesis of Gallium(III)-pyridine-5,15-4-t-butylphenyl-10-pyrenyl-ethynylcorrole (7 b): Gallium corrole **6 a** was cross-coupled, according to the general procedure for the Sonogashira cross-coupling reaction utilizing 1.1 equiv. iodopyrene. Purification was accomplished *via* column chromatography (aluminium oxide 60, basic, activity level II, DCM + 1 % pyridine) and the product **7 b** was obtained as a green solid (40 mg, 63 %). ^{1}H-NMR (300 MHz, $CDCl_3$, 25 °C): δ = 9.64 (d, J(H,H) = 4.5 Hz, 2 H, pyrrole-H), 9.35 (d, J(H,H) = 9.0, 1 H, pyrene-H), 9.21 (d, J(H,H) = 4.4 Hz, 2 H, pyrrole-H), 9.04 (d, J(H,H) = 3.8 Hz, 2 H, pyrrole-H), 8.83 (d, J(H,H) = 3.8 Hz, 2 H, pyrrole-H), 8.70 (d, J(H,H) = 7.9, 1 H, pyrene-H), 8.00–8.36 (m, 11 H, pyrene-H), 7.86 (d, J(H,H) = 8.0, 4 H, phenyl-H), 6.86–6.91 (m, 1 H, pyridine-H), 6.17–6.21 (m, 2 H, pyridine-H), 4.38 (s, 2 H, pyridine-H), 1.65 (s, 18 H, CH_3); ^{13}C-NMR (125 MHz, $CDCl_3$, 25 °C): δ = 150.1, 147.2, 145.5, 140.7, 138.2, 137.6, 135.7, 134.4, 131.5, 130.5, 129.6, 129.4, 128.2, 127.4, 126.2, 125.3, 124.9, 124.5, 123.8, 123.3, 119.0, 115.6, 99.1, 93.2, 88.2, 34.9, 31.7; HRMS *m/z*: calcd. For $C_{62}H_{47}GaN_5^-$: 930.3093 [*M*–H]$^-$; found 929.2919; λ_{max} nm (log ε): 243 (4.96), 286 (4.82), 454 (5.32), 473 (5.34), 547 (4.39), 594 (4.59), 633 (4.61) ; Emission λ_{max} = 648 nm.

Synthesis of Gallium(III)-pyridine-5,15-4-t-butylphenyl-10-(4-t-butylphenylethynyl)corrole (7 c): Gallium corrole **6 a** was cross-coupled, according to the general procedure for the Sonogashira cross-coupling reaction utilizing 1.1 equiv. 4-t-butyliodobenzene. Purification was accomplished *via* column chromatography (aluminium oxide 60, basic, activity level II, DCM + 1 % pyridine) and the product **7 c** was obtained (30 mg, 51 %). ^{1}H-NMR (300 MHz, $CDCl_3$, 25 °C): δ = 9.42 (d, J(H,H) = 4.5 Hz, 2 H, pyrrole-H), 9.13 (d, J(H,H) = 4.5 Hz, 2 H, pyrrole-H), 9.02 (d, J(H,H) = 3.9 Hz, 2 H, pyrrole-H), 8.81 (d, J(H,H) = 3.9 Hz, 2 H, pyrrole-H), 8.27 (d, J(H,H) = 8.1 Hz, 4 H, phenyl-H), 7.94 (d, J(H,H) = 8.2 Hz, 2 H, phenyl-H), 7.84 (d, J(H,H) = 8.1 Hz, 4 H, phenyl-H), 7.58 (d, J(H,H) = 8.2, 2 H, phenyl-H), 7.38–7.44 (m, 1 H, phenyl-H), 7.11 (t, J(H,H) = 6.9 Hz, 1 H, pyridine-H), 6.52 (s, 2 H, pyridine-H), 5.73 (s, 2 H, pyridine-H), 1.64 (s, 18 H, CH_3); ^{13}C-NMR (75 MHz, $CDCl_3$, 25 °C): δ = 150.7, 149.9, 147.1, 146.0, 140.6, 138.3, 137.5, 137.3, 135.5, 134.3, 131.1, 126.0, 125.6, 124.5, 123.7, 123.3, 122.1, 118.6, 115.5, 93.4, 91.9, 88.1, 34.8, 31.7, 31.3; HRMS m/z: calcd. for $C_{56}H_{51}GaN_5^-$: 862.3406 [M–H]$^-$; found 861.3245; λ_{max} nm (log ε): 291 (4.39), 444 (5.32), 540 (4.07), 579 (4.04), 628 (4.35); Emission λ_{max} = 640 nm.

Synthesis of Gallium(III)-pyridine-5,15-4-t-butylphenyl-10-(4-nitro-phenylethynyl)corrole (7 d): Gallium corrole **6 a** was cross-coupled, according to the general procedure for the Sonogashira cross-coupling reaction utilizing 1.1 equiv. 1-iodo-4-nitrobenzene. Purification was accomplished *via* column chromatography (alumi-

nium oxide 60, basic, activity level II„ DCM + 1% pyridine) and the product **7d** was obtained (12 mg, 21%). ^{1}H-NMR (300 MHz, $CDCl_3$, 25 °C): δ = 9.30 (d, J(H,H) = 4.5 Hz, 2 H, pyrrole-H), 9.13 (d, J(H,H) = 4.6 Hz, 2 H, pyrrole-H), 8.99 (d, J(H,H) = 3.9 Hz, 2 H, pyrrole-H), 8.79 (d, J(H,H) = 3.9 Hz, 2 H, pyrrole-H), 8.23–8.27 (m, 6 H, phenyl-H), 7.83–7.88 (m, 6 H, phenyl-H), 6.93–6.98 (m, 1 H, pyridine-H), 6.22–6.26 (m, 2 H, pyridine-H), 4.53 (s, 2 H, pyridine-H), 1.64 (s, 18 H, CH_3); ^{13}C-NMR (125 MHz, $CDCl_3$, 25 °C): δ = 150.2, 147.4, 145.7, 144.4, 140.4, 138.2, 138.0, 137.6, 136.1, 134.3, 132.1, 130.8, 129.8, 128.7, 126.6, 125.6, 124.6, 123.9, 122.7, 120.0, 115.8, 100.3, 93.2, 86.3, 34.9, 31.7; HRMS *m/z*: calcd. for $C_{52}H_{42}GaN_6O_2^-$: 851.2631 [*M*−H]$^-$; found 850.2483; λ_{max} nm (log ε): 294 (4.27), 425 (4.77), 458 (4.60), 493 (4.48), 576 (4.09), 617 (4.27); Emission λ_{max} = 615 nm.

General procedure for the two-fold Sonogashira cross-coupling reaction in the flow-reactor: Solution A [**6b** (0.601 mmol), $Pd(PPh_3)_4$ (76 mg, 5 mol%), CuI (20 mg, 8 mol%) and Hünig's base (682 µL, 3 equiv.) dissolved in 37.5 mL DMF] and solution B [corresponding aryliodide (4.4 equiv.) dissolved in 2.6 mL DMF] were mixed (solution A: flow rate 1 mL/min, V = 5 mL; solution B: 0.2 mL/min, V = 1.3 mL) and fed into the reactor (reactor volume = 10 mL, T = 80 °C, residence time = 10 min). The collected product was filtered *via* Celite with EtOAc as solvent, followed by concentration under vacuum.

Synthesis of Gallium(III)-pyridine-5,15-phenylethynyl-10-(4-t-butyl-phenyl)corrole (8a): Gallium corrole **6b** was cross-coupled, according to the general procedure for the Sonogashira cross-coupling reaction utilizing 2.2 equiv. iodobenzene. Purification was accomplished *via* column chromatography (aluminium oxide 60, basic, activity level II, DCM + 1% pyridine) and the product **8a** was obtained (30 mg, 48%). ^{1}H-NMR (300 MHz, $CDCl_3$, 25 °C): δ = 9.60 (d, J(H,H) = 4.5 Hz, 2 H, pyrrole-H), 9.38 (d, J(H,H) = 3.7 Hz, 2 H, pyrrole-H), 9.15 (d, J(H,H) = 3.8 Hz, 2 H, pyrrole-H), 8.86 (d, J(H,H) = 4.4 Hz, 2 H, pyrrole-H), 8.12 (d, J(H,H) = 8.0 Hz, 2 H, phenyl-H), 8.00 (d, J(H,H) = 7.3 Hz, 4 H, phenyl-H), 7.80 (d, J(H,H) = 8.1 Hz, 2 H, phenyl-H), 7.49–7.56 (m, 4 H, phenyl-H), 7.42–7.46 (m, 2 H, phenyl-H), 6.87 (t, J(H,H) = 7.7 Hz, 1 H, pyridine-H), 6.16–6.21 (m, 2 H, pyridine-H), 4.50 (d, J(H,H) = 4.8 Hz, 2 H, pyridine-H), 1.65 (s, 9 H, CH_3); ^{13}C-NMR (125 MHz, $CDCl_3$, 25 °C): δ = 149.9, 144.5, 144.2, 143.6, 139.6, 138.9, 138.1, 135.1, 134.2, 132.2, 131.9, 131.5, 128.6, 127.9, 126.7, 126.0, 124.5, 124.1, 123.8, 116.8, 113.5, 95.4, 95.0, 91.7, 34.9, 31.8; HRMS *m/z*: calcd. for $C_{50}H_{35}GaN_5^-$: 774.2154 [*M*−H]$^-$; found 773.2000; λ_{max} nm (log ε): 309 (4.27), 446 (5.21), 470 (4.76), 560 (3.88), 612 (4.22), 664 (4.81). Emission λ_{max} = 676 nm.

Synthesis of Gallium(III)-pyridine-5,15-pyrenylethynyl-10-(4-t-butylphenyl)corrole (8b): Gallium corrole **6b** was cross-coupled, according to the general procedure for the Sonogashira cross-coupling reaction utilizing 2.2 equiv. iodopyrene. Purification was accomplished *via* column chromatography (aluminium oxide 60, basic, activity level II, DCM + 1% pyridine) and the product **8b** was obtained (56 mg, 68%). ^{1}H-NMR (300 MHz, $CDCl_3$, 25 °C): δ = 9.78 (s, 2 H, pyrrole-H), 9.39 (s, 2 H, pyrrole-H), 9.11 (d, J(H,H) = 8.8 Hz, 2 H, pyrene-H), 8.94 (s, 4 H, pyrrole-H), 8.34–8.37 (m, 2 H, pyrene-H), 8.23–8.25 (m, 2 H, pyrene-H), 8.08–8.11 (m, 2 H, pyrene-H), 7.36–7.94 (m, 14 H, pyrene-H), 6.73 (t, J(H,H) = 7.69 Hz, 1 H, pyridine-H), 6.07 (t, J(H,H) = 6.41 Hz, 2 H, pyridine-H), 4.46–4.47 (m, 2 H, pyridine-H), 1.73 (s, 9 H, CH_3); ^{13}C-NMR (125 MHz, $CDCl_3$, 25 °C): δ = 149.9, 144.5, 144.1, 143.3, 139.4, 139.1, 137.9, 134.6, 134.4, 132.0, 131.1, 130.9, 130.2, 129.1, 128.4, 127.8, 127.2, 126.7, 125.7, 125.0, 124.2, 123.9, 123.6, 119.1, 116.6, 98.2, 95.6, 95.4, 31.9; HRMS m/z: calcd. for $C_{70}H_{43}GaN_5^-$: 1022.2780 [*M*−H]$^-$; found 1021.2195; λ_{max} nm (log ε): 244 (4.92), 277 (4.65), 325 (4.50), 475 (5.17), 637 (4.34), 695 (4.90). Emission λ_{max} = 712 nm.

Synthesis of Gallium(III)-pyridine-5,15-(4-t-butylphenylethynyl)-10-(4-t-butylphenyl)corrole (8c): Gallium corrole **6b** was cross-coupled, according to the general procedure for the Sonogashira cross-coupling reaction utilizing 2.2 equiv. 4-t-butyliodobenzene. Purification was accomplished *via* column chromatography (aluminium oxide 60, basic, activity level II, DCM + 1% pyridine) and the product **8c** was obtained (15 mg, 21%). ^{1}H-NMR (300 MHz, $CDCl_3$, 25 °C): δ = 9.59 (d, J(H,H) = 4.4 Hz, 2 H, pyrrole-H), 9.37 (d, J(H,H) = 3.7 Hz, 2 H, pyrrole-H), 9.16 (d, J(H,H) = 3.8 Hz, 2 H, pyrrole-H), 8.83 (d, J(H,H) = 4.4 Hz, 2 H, pyrrole-H), 8.11 (d, J(H,H) = 8.0 Hz, 2 H, phenyl-H), 7.98 (d, J(H,H) = 8.2 Hz, 4 H, phenyl-H), 7.78 (d, J(H,H) = 8.0 Hz, 2 H, phenyl-H), 7.60 (d, J(H,H) = 8.2 Hz, 4 H, phenyl-H), 6.71–6.75 (m, 1 H, pyridine-H), 5.95–5.99 (m, 2 H, pyridine-H), 3.60 (s, 2 H, pyridine-H), 1.63 (s, 9 H, CH_3), 1.47 (s, 18 H, CH_3); ^{13}C-NMR (125 MHz, $CDCl_3$, 25 °C): δ = 151.3, 149.9, 144.5, 143.7, 143.1, 139.6, 138.9, 138.6, 135.0, 134.2, 131.3, 126.8, 125.9, 125.6, 124.5, 124.1, 123.8, 121.7, 116.7, 113.2, 95.5, 95.3, 90.9, 34.9, 31.7, 31.3; HRMS *m/z*: calcd. for $C_{58}H_{51}GaN_5^-$: 886.3406 [*M*−H]$^-$; found 885.3245; λ_{max} nm (log ε): 306 (4.43), 446 (5.21), 473 (4.74), 555 (4.03), 612 (4.28), 667 (4.75). Emission λ_{max} = 678 nm.

Synthesis of Gallium(III)-pyridine-5,15-(4-nitrophenylethynyl)-10-(4-t-butylphenyl)corrole (8d): Gallium corrole **6b** was cross-coupled, according to the general procedure for the Sonogashira cross-coupling reaction utilizing 2.2 equiv. 1-iodo-4-nitrobenzene. Purification was accomplished *via* column chromatography (aluminiumoxide 60, basic, acitivity level II, DCM + 1% pyridine) and the product **8d** was obtained (38 mg, 55%). ^{1}H-NMR (300 MHz, $CDCl_3$, 25 °C): δ = 9.37 (d, J(H,H) = 4.6 Hz, 2 H, pyrrole-H), 9.17 (s, 4 H, pyrrole-H), 8.91 (d, J(H,H) = 4.6 Hz, 2H, pyrrole-H), 8.22 (d, J(H,H) = 8.1 Hz, 2 H, phenyl-H), 7.89 (d, J(H,H) = 8.1 Hz, 2 H, phenyl-H), 7.78 (d, J(H,H) = 8.1 Hz, 2 H, phenyl-H), 7.33 (d, J(H,H) = 8.3 Hz, 2 H, phenyl-H), 6.97–6.92 (m, 3 H, pyridine-H), 6.30–6.83 (m, 3 H, pyridine-H), 4.83 (s, 3 H, pyridine-H), 1.70 (s, 9 H, CH3); ^{13}C-NMR (125 MHz, $CDCl_3$, 25 °C): δ = 150.4, 145.6, 145.1, 144.8, 143.2, 140.0, 138.6, 137.9, 134.2, 132.0, 131.9, 130.7, 128.5, 128.4, 126.6, 125.1, 124.3, 123.8, 123.2, 117.5, 115.2, 97.7, 94.2, 93.7, 35.0, 31.8; HRMS *m/z*: calcd. for $C_{52}H_{42}GaN_6O_2^-$: 864.1855 [*M*−H]$^-$; found 863.1697; λmax nm (log ε): 294 (4.42), 425 (4.69), 488 (4.93), 637 (4.36), 690 (4.95); Emission λ_{max} = 723 nm.

General procedure for the three-fold Sonogashira cross-coupling reaction in the flow-reactor: Solution A [**6c** (0.470 mmol), $Pd(PPh_3)_4$ (120 mg, 5 mol%), CuI (32 mg, 8 mol%) and Hünig's base (1082 µL, 3 equiv.) dissolved in 33 mL DMF] and solution B [corresponding aryliodide (6.6 equiv.) dissolved in 2.6 mL DMF] were mixed (solution A: flow rate 1 mL/min, V = 5 mL; solution B: 0.2 mL/min, V = 1.3 mL) and fed into the reactor (reactor volume = 10 mL, T = 80 °C, residence time = 10 min). The collected product was filtered *via* Celite with EtOAc as solvent, followed by concentration under vacuum.

Synthesis of gallium(III)-pyridine-5,10,15-phenylethynyl-corrole (9a): Gallium corrole **6c** was cross-coupled according to the general procedure for the three-fold Sonogashira cross-coupling reaction in the flow-reactor utilizing 3.3 equiv. iodobenzene. Purification was accomplished *via* column chromatography (aluminium oxide 60, basic, activity level II, DCM + 10% pyridine) and the product **9a** was obtained as a green solid (23 mg, 31%). ^{1}H-NMR (500 MHz, $CDCl_3$, 25 °C): δ = 9.55 (d, J(H,H) = 4.7 Hz, 2 H, pyrrole-H), 9.39 (d, J(H,H) = 4.5 Hz, 2 H, pyrrole-H), 9.25 (d, J(H,H) = 3.8 Hz, 2 H, pyrrole-H), 8.99 (d, J(H,H) = 3.8 Hz, 2 H, pyrrole-H), 7.97–7.99 (m, 6 H, phenyl-H), 7.50–7.53 (m, 6 H, phenyl-H), 7.41–7.44 (m, 3 H, phenyl-H), 6.93 (t, J(H,H) = 7.4 Hz, 1 H, pyridine-H), 6.26 (t, J(H,H) = 6.6 Hz, 2 H, pyridine-H), 4.71 (s, 2 H, pyridine); ^{13}C-NMR (175 MHz, $CDCl_3$, 25 °C): δ = 145.6, 144.4, 143.7, 139.4, 138.2, 135.7, 131.6, 131.4, 128.6, 127.8, 127.4, 125.1, 124.3, 123.9, 116.9, 96.0, 94.5, 92.0, 91.7, 91.1; HRMS *m/z*: calcd. for $C_{43}H_{24}GaN_4$: 664.1179 [*M*-pyr + H]; found 664.1191; λ_{max} nm (log ε): 416 (5.80), 517 (4.60), 571 (4.63), 626 (4.22); Emission λ_{max} = 699, 761 nm.

Synthesis of Gallium(III)-pyridine-5,10,15-pyrenylethynyl-corrole (9b): Gallium corrole **6c** was cross-coupled according to the general procedure for the three-fold Sonogashira cross-coupling reaction in the flow-reactor utilizing 3.3 equiv. iodopyrene. Purification was accomplished *via* column chromatography (aluminium oxide 60, basic, activity level II, DCM + 10% pyridine) and the product **9a** was obtained as a green solid as a purple solid (22 mg, 49%). $R_f = 0.69$ (DCM/heptane (1:1) + 10% pyridine); ^{1}H-NMR (700 MHz, $CDCl_3$, 25 °C): $\delta = 9.52$ (d, J(H,H) = 3.7 Hz, 2 H, pyrrole-H), 9.27 (d, J(H,H) = 2.9 Hz, 4 H, pyrrole-H), 9.19 (t, J(H,H) = 8.2 Hz, 3 H, pyrenyl-H), 8.85 (d, J(H,H) = 2.9 Hz, 2 H, pyrrole-H), 8.52 (d, J(H,H) = 7.2 Hz, 1 H, pyrenyl-H), 8.49 (d, J(H,H) = 7.2 Hz, 2 H, pyrenyl-H), 8.34 (d, J(H,H) = 8.6 Hz, 1 H, pyrenyl-H), 8.27 (d, J(H,H) = 8.5 Hz, 2 H, pyrenyl-H), 8.11 (d, J(H,H) = 6.9 Hz, 3 H, pyrenyl-H), 8.08 (d, J(H,H) = 7.0 Hz, 2 H, pyrenyl-H), 8.03 (d, J(H,H) = 7.2 Hz, 1 H, pyrenyl-H), 7.98–8.01 (m, 3 H, pyrenyl-H), 7.92–7.95 (m, 4 H, pyrenyl-H), 7.90 (t, J(H,H) = 7.0 Hz, 1 H, pyrenyl-H), 7.83–7.85 (m, 3 H, pyrenyl-H), 7.80–7.81 (m, 1 H, pyrenyl-H), 6.87 (bs, 1 H, pyridine-H), 6.21 (bs, 2 H, pyridine-H), 4.97 (bs, 2 H, pyridine-H); ^{13}C-NMR (176 MHz, $CDCl_3$, 25 °C): $\delta = 145.1$, 143.5, 139.2, 138.0, 135.4, 132.2, 131.6, 131.5, 131.4, 131.3, 131.3, 130.8, 130.6, 129.7, 129.6, 128.7, 128.7, 128.4, 128.3, 127.8, 127.5, 127.3, 126.3, 126.2, 126.1, 125.5, 125.5, 125.4, 125.3, 125.1, 124.8, 124.7, 124.6, 124.5, 124.5, 124.2, 123.9, 119.8, 119.4, 116.7, 101.3, 98.4, 98.0, 97.6, 96.2, 94.8, 92.7; MS *m/z*: calcd. for $C_{73}H_{36}GaN_4^+$: 1037.2196 [*M*-pyr + H]$^+$; found 1037.2189; UV-Vis (DCM, nm) λ_{max} (log ε): 334 (4.11), 403 (3.92), 502 (4.69), 588 (3.64), 643 (3.76), 713 (4.19); Emission $\lambda_{max} = 740$, 816 nm.

Synthesis of Gallium(III)-pyridine-5,10,15-(4-nitrophenyl-ethynyl)-corrole (9d): Gallium corrole **6c** was cross-coupled according to the general procedure for the three-fold Sonogashira cross-coupling reaction in the flow-reactor utilizing 3.3 equiv. 1-iodo-4nitrobenzene. Purification was accomplished *via* column chromatography (aluminium oxide 60, basic, activity level II, DCM + 10% pyridine) and the product **9a** was obtained as a green solid (17 mg, 42%). ^{1}H-NMR (300 MHz, $CDCl_3$, 25 °C): $\delta = 9.51$ (d, J(H,H) = 3.7 Hz, 2 H, pyrrole-H), 9.35 (d, J(H,H) = 3.7 Hz, 2 H, pyrrole-H), 9.26 (d, J(H,H) = 3.7 Hz, 3 H, pyrrole-H), 9.09 (d, J(H,H) = 3.7 Hz, 2 H, pyrrole-H), 8.35–8.39 (m, 6 H, phenyl-H), 8.00–8.06 (m, 6 H, phenyl-H), 6.91 (bs, 1 H, pyridine-H), 6.30 (bs, 2 H, pyridine-H), 3.61 (d, J(H,H) = 14.5 Hz, 2 H, pyridine-H); HRMS *m/z*: calcd. for $C_{48}H_{25}GaN_8O_6$: 844.0707 [M-pyr + HCOO]$^-$; found: 844.0719 [M-pyr + HCOO]$^-$; UV-Vis (DCM, nm) λ_{max} (log ε): 228 (3.43), 293 (3.23), 416 (3.24), 529 (3.67), 653 (3.03), 713 (3.37); Emission $\lambda_{max} = 717$ nm.

DFT Calculations: All calculations were performed using the Gaussian 09 package version EM64L–G09RevC.01.[55] Electronic structure calculations were based on Kohn-Sham density functional theory (KS-DFT) with Becke's three-parameter hybrid functional (B3LYP)[56,57] and a compound basis set, where the Pople's 6–311 + G(d,p) basis sets were used for C, H, N, O, Ga.[58,59] For our system, we first performed a tight structural optimization, followed by a frequency calculation to confirm that the optimized structure was indeed a minimum (with no imaginary frequencies). To gain insight into the vertical singlet electronic states, time-dependent density functional theory[60] (with B3LYP, CAM-B3LYP, and PBE0 hybrid functionals) calculations were performed.

Acknowledgements

W.S. acknowledges the financial support from the Austrian Science Foundation (FWF) (FWF-P28167-N34 and FWF-P32045-NBL). The NMR spectrometers were acquired in collaboration with the University of South Bohemia (CZ) with financial support from the European Union through the EFRE INTERREG IV ETC-AT-CZ program (project M00146, "RERI-uasb"). M.H. and W.S. thanks Dr. Markus Himmelsbach and DI Thomas Bögl for the ESI-MS measurement.

Conflict of Interest

The authors declare no conflict of interest.

Keywords: Corroles · Cross-coupling · Gallium · NIR emitter · Nitrogen heterocycles

[1] Z. Gross, N. Galili, *Angew. Chem. Int. Ed.* **1999**, *38*, 2366–2369.
[2] D. T. Gryko, K. Jadach, *J. Org. Chem.* **2001**, *66*, 4267–4275.
[3] B. Koszarna, D. T. Gryko, *J. Org. Chem.* **2006**, *71*, 3707–3717.
[4] S. M. Borisov, A. Alemayehu, A. J. Ghosh, *J. Mater. Chem. C* **2016**, *4*, 5822.
[5] R. Paolesse, S. Nardis, D. Monti, M. Stefanelli, C. Di Natale, *Chem. Rev.* **2017**, *117*, 2517–2583.
[6] C. M. Lemon, D. C. Powers, P. J. Brothers, D. G. Nocera, *Inorg. Chem.* **2017**, *56*, 10991–10997.
[7] I. Aviv-Harel, Z. Gross, *Chem. Eur. J.* **2009**, *15*, 8382–8394.
[8] W. Schöfberger, F. Faschinger, S. Chattopadhyay, S. Bhakta, B. Mondal, J. A. A. W. Elemans, S. Müllegger, S. Tebi, R. Koch, F. Klappenberger, M. Paszkiewicz, J. V. Barth, E. Rauls, H. Aldahhak, W. G. Schmidt, A. Dey, *Angew. Chem. Int. Ed.* **2016**, *55*, 2350–2355.
[9] R. D. Teo, J. Y. Hwang, J. Termini, Z. Gross, H. B. Gray, *Chem. Rev.* **2017**, *117*, 2711–2729.
[10] S. Gonglach, S. Paul, M. Haas, F. Pillwein, S. S. Sreejith, S. Barman, R. De, S. Mülleger, P. Gerschel, U. P. Apfel, H. Coskun, A. Aljabour, P. Stadler, S. Roy, W. Schöfberger, *Nat. Commun.* **2019**, *10*, 3864–3874.
[11] J. F. B. Barata, M. G. P. M. S. Neves, M. A. F. Faustino, A. C. Tomé, J. A. S. Cavaleiro, *Chem. Rev.* **2017**, *117*, 3192–3253.
[12] R. Orłowski, D. Gryko, D. T. Gryko, *Chem. Rev.* **2017**, *117*, 3102–3137.
[13] M. Stefanelli, M. Mastroianni, S. Nardis, S. Licoccia, F. R. Fronczek, K. M. Smith, W. Zhu, Z. Ou, K. M. Kadish, R. Paolesse, *Inorg. Chem.* **2007**, 46, 10791–10799.
[14] M. Schmidlehner, F. Faschinger, L. M. Reith, M. Ertl, W. Schoefberger, *Appl. Organomet. Chem.* **2013**, *27*, 395–405.
[15] M. König, L. M. Reith, U. Monkowius, G. Knör, K. Bretterbauer, W. Schöfberger, *Tetrahedron* **2011**, *67*, 4243–4252.
[16] M. Tiffner, S. Gonglach, M. Haas, W. Schöfberger, M. Waser, *Chem. Asian J.* **2017**, *12*, 1048–1051.
[17] W. Sinha, M. G. Sommer, N. Deibel, F. Ehret, B. Sarkar, S. Kar, *Chem. Eur. J.* **2014**, *20*, 15920–15932.
[18] D. T. Gryko, *Eur. J. Org. Chem.* **2002**, *11*, 1735–1743.
[19] M. Haas, S. Gonglach, S. Muellegger, W. Schöfberger, *Monatsh. Chem.* **2018**, *149*, 773–781.
[20] M. Haas, S. Gonglach, W. Schöfberger, *J. Porphyrins Phthalocyanines* **2019**, *23*, 1–13.
[21] K. Ueta, K. Naoda, S. Ooi, T. Tanaka, A. Osuka, *Angew. Chem. Int. Ed.* **2017**, *56*, 7223–7226.
[22] J. Bendix, I. J. Dmochowski, H. B. Gray, A. Mahammed, L. Simkhovich, Z. Gross, *Angew. Chem. Int. Ed.* **2000**, *39*, 4048–4051.
[23] V. S.-Y. Lin, S. G. DiMagno, M. J. Therien, *Science* **1994**, *264*, 1105–1111.
[24] V. S.-Y. Lin, M. J. Therien, *Chem. Eur. J.* **1995**, *1*, 645–651.
[25] P. J. Angiolillo, H. T. Uyeda, T. V. Duncan, M. J. Therien, *J. Phys. Chem. B* **2004**, *108*, 11893–11903.
[26] J. C. Ostrowski, K. Susumu, M. R. Robinson, M. J. Therien, G. C. Bazan, *Adv. Mater.* **2003**, *15*, 1296–1300.
[27] P. N. Taylor, J. Huuskonen, G. Rumbles, R. T. Aplin, E. Williams, H. L. Anderson, *Chem. Commun.* **1998**, *8*, 909–910.
[28] K. Nakamura, T. Fujimoto, S. Takara, K.-I. Sugiura, H. Miyasaka, T. Ishii, M. Yamashita, Y. Sakata, *Chem. Lett.* **2003**, *32*, 694–695.
[29] H. L. Anderson, S. J. Martin, D. D. C. Bradley, *Angew. Chem. Int. Ed. Engl.* **1994**, *33*, 655–657.
[30] A. Osuka, N. Tanabe, S. Kawabata, I. Yamazaki, Y. Nishimura, *J. Org. Chem.* **1996**, *60*, 7177–7185.
[31] K. Maruyama, S. Kawabata, *Bull. Chem. Soc. Jpn.* **1990**, *63*, 170–175.
[32] P. N. Taylor, H. L. Anderson, *J. Am. Chem. Soc.* **1999**, *121*, 11538–11545.

[33] A. M. Shulga, G. V. Ponomarev, *Chem. Heterocycl. Compd.* **1988**, *24*, 276–280.
[34] M. Chachisvilis, V. S. Chirvony, A. M. Shulga, B. Källebring, S. Larsson, V. Sundström, *J. Phys. Chem.* **1996**, *100*, 13857–13866.
[35] H. L. Anderson, *Tetrahedron Lett.* **1992**, *33*, 1101–1104.
[36] W. Ehrfeld, V. Hessel, H. Lowe, *Microreactors: New Technology for Modern Chemistry*, Wiley-VCH: Weinheim, **2000**.
[37] K. Geyer, J. D. C. Codée, P. H. Seeberger, *Chem. Eur. J.* **2006**, *12*, 8434–8442.
[38] T. Fukuyama, M. Shinmen, S. Nishtani, M. Sato, I. Ryu, *Org. Lett.*, **2002**, *4*, 1691–1694.
[39] D. T. Gryko, *J. Porphyrins Phthalocyanines*, **2008**, *12*, 906–917.
[40] C. Würth, M. Grabolle, J. Pauli, M. Spieles, U. Resch-Genger, *Nat. Protoc.* **2013**, *8*(10), 1535–1550.
[41] P. G. Seybol, M. Gouterman, *J. Mol. Spectrosc.* **1969**, *31*, 1–13.
[42] S. M. LeCours, S. G. DiMagno, M. J. Therien, *J. Am. Chem. Soc.* **1996**, *118*, 11854–11864.
[43] V. S. Lin, S. G. DiMagno, M. J. Therien, *Science* **1994**, *264*, 1105–1111.
[44] L. R. Milgrom, G. Yahioglu, *Tetrahedron Lett.* **1995**, *36*, 9061–9064.
[45] M. Uttamlal, A. S. Holmes-Smith, *Chem. Phys. Lett.* **2008**, *454*, 223–228.
[46] V. N. Knyukshto, E. Zenkevich, E. Sagun, A. Shulga, S. M. Bachilo, *Chem. Phys. Lett.* **1999**, *304*, 155–166.
[47] V. Knyukshto, É. I. Zen'kevich, E. I. Sagun, A. M. Shul'ga, S. M. Bachilo, *J. Appl. Spectrosc.* **1999**, *66*, 588–592.
[48] V. N. Knyukshto, E. I. Sagun, A. M. Shul'ga, S. M. Bachilo, E. I. Zen'kevich, *Opt. Spectrosc.* **2000**, *88*, 205–216.
[49] S. Dahal, V. Krishnan, *J. Photochem. Photobiol. A* **1995**, *89*, 105–112.
[50] S. Dahal, V. Krishnan, *Chem. Phys. Lett.* **1997**, *274*, 390–395.
[51] D. K. Dogutan, S. H. H. Zaidi, P. Thamyongkit, J. S. Lindsey, *J. Org. Chem.* **2007**, *72*(20), 7701–7714.
[52] N. S. Hush, J. M. Dyke, M. L. Williams, I. S. Woolsey, *J. Chem. Soc. Dalton Trans.* **1974**, 395.
[53] A. Ghosh, T. Wondimagegn, A. B. J. Parusel, *J. Am. Chem. Soc.* **2000**, *122*, 5100.
[54] G. A. Brito, F. Della-Felice, G. Luo, A. S. Burns, R. A. Pilli, S. D. Rychnovsky, M. J. Krische, *Org. Lett.* **2018**, *20*(13), 4144–4147.
[55] M. J. Frisch, et al.; Gaussian, Inc.: Wallingford, CT, **2009**.
[56] C. Lee, W. Yang, R. G. Parr, *Phys. Rev. B* **1988**, *37*, 785.
[57] A. D. Becke, *J. Chem. Phys.* **1993**, *98*, 5648.
[58] M. J. Frisch, J. A. Pople, J. S. Binkley, *J. Chem. Phys.* **1984**, *80*, 3265.
[59] W. R. Wadt, P. J. Hay, *J. Phys. Chem.* **1985**, *82*, 284.
[60] M. E. Casida, C. Jaorski, K. C. Casida, D. R. Salahub, *J. Chem. Phys.* **1998**, *108*, 4439.

Manuscript received: January 27, 2021
Revised manuscript received: January 29, 2021
Accepted manuscript online: February 4, 2021